Arabian Journal of Chemistry (2022) **15**, 103939

King Saud University

Arabian Journal of Chemistry

www.ksu.edu.sa
www.sciencedirect.com

ORIGINAL ARTICLE

Investigation of fragmentation behaviors of steroidal drugs with Li^+, Na^+, K^+ adducts by tandem mass spectrometry aided with computational analysis

Adeeba Khadim [a], Syed Usama Yaseen Jeelani [a], Naheed Akhtar [a], Arslan Ali [b], Syed Mohammad Zaki Shah [a], Bibi Zareena [a], Syeda Tehreem [a], Jalal Uddin [d], Hesham R. El-Seedi [e,f,g], Syed Ghulam Musharraf [a,b,c,*]

[a] *H.E.J. Research Institute of Chemistry, International Center for Chemical and Biological Sciences, University of Karachi, Karachi 75270, Pakistan*
[b] *Dr. Panjwani Center for Molecular Medicine and Drug Research, International Center for Chemical and Biological Sciences, University of Karachi, Karachi 75270, Pakistan*
[c] *T.C.M. Hospital of Southwest Medical University, Luzhou 646000, China*
[d] *Department of Pharmaceutical Chemistry, College of Pharmacy, King Khalid University, Abha 62529, Saudi Arabia*
[e] *Department of Molecular Biosciences, The Wenner-Gren Institute, Stockholm University, SE-106 91 Stockholm, Sweden*
[f] *Department of Chemistry, Faculty of Science, Menoufia University, Shebin El-Kom 32512, Egypt*
[g] *International Research Center for Food Nutrition and Safety, Jiangsu University, Zhenjiang 212013, China*

Received 1 March 2022; accepted 20 April 2022
Available online 26 April 2022

KEYWORDS

Drugs;
Metal adducts;
Fragmentation;
ESI-MS/MS;
Computational studies

Abstract In this study, we have investigated the fragmentation of the widely used steroidal pharmaceutical drugs (n = 14), complexed by a singly charged proton or alkali metal ion (Li^+, Na^+, K^+) using Ion trap and quadrupole time-of-flight mass spectrometers. Spectra were collected by LC-MS/MS analysis using system automated collision energy i.e., of 25–60 eV. Theoretical calculations were also calculated using DFT software. The metal complexes showed different fragmentation pathways not commonly observed for protonated compounds. There was a distinct difference observed in the relative intensities of some common fragments for free vs. metallated drugs. Some major fragments from protonated and lithium adducts showed close resemblance, while sodium and

* Corresponding author at: H.E.J. Research Institute of Chemistry, International Center for Chemical and Biological Sciences, University of Karachi, Karachi 75270, Pakistan.
E-mail address: musharraf1977@yahoo.com (S. Ghulam Musharraf).
Peer review under responsibility of King Saud University.

Production and hosting by Elsevier

https://doi.org/10.1016/j.arabjc.2022.103939

potassium adducts showed different fragments. Theoretical calculations showed a distinct difference in the position of attachment of proton and metals. This adducts ion fragmentation information will be helpful for the identification of these compounds in complex samples.

1. Introduction

Liquid chromatography-electrospray mass spectrometry (LC-ESI-MS) has been applied to the analysis and structural characterization of various compounds, including peptides (Lee et al., 1998, Wang et al., 2006), proteins (Wang et al., 2006, Perdivara et al., 2009), polymers (Perdivara et al., 2009), lipids (El-Aneed et al., 2007), and organic molecules (Kim et al., 1996, Fang et al., 2020). Structures of unknown drug-related compounds can be deduced by comparing their fragmentation patterns with standard drugs (Zhu et al., 2011, Kasper et al., 2012, Nikolskiy et al., 2015). With the growth of the pharmaceutical industry, structural elucidation of drugs and their derivatives using tandem mass spectrometry (MS2) has become essential for drug development and pharmacokinetics studies due to its high sensitivity and low sample requirement. Identification of desired compounds is hindered in complex samples such as urine, plasma, and plant extracts due to a high amount of salt. Different metal adduct ions may be formed during ESI-MS depending on the nature of the compound, solvent, and ESI parameters (Cech and Enke 2001). Interactions of metal cations facilitate the ionization of organic molecules devoid of basic and acidic functional groups via ESI ionization (Kruve et al., 2013, Liigand et al., 2020). In addition, to enhance the ionization efficiency, alkali metal cations can induce unique dissociation and fragmentation pathways of the ions by specific interactions with functional groups followed by structural rearrangements (Selby et al., 1994, Duan et al., 2012, Fujihara et al., 2014, Wei et al., 2015, Hong et al., 2017). This fragmentation pattern will help for structure elucidation and the quantification of drugs. The most common adducts ions formed in positive ionization mode are sodium and potassium (Bacaloni et al., 2005). Alkali metal ions' size and binding properties uniquely affect their structural rearrangements and fragmentation patterns (Selby et al., 1994, Fujihara et al., 2014, Hong et al., 2017). The distinct fragmentation pathways and related gas-phase structures of drugs complexed with different alkali metal cations enable their identification based on MS/MS analysis of these species.

Research seeking fundamental insight into the relationship between fragmentation patterns and gas-phase precursor structure has gained attention (Fragkaki et al., 2009, Musharraf et al., 2013, Uddin et al., 2022). The investigation of the fragmentation mechanism and structural characterization of the protonated molecular ions of the drugs using collision-induced dissociation (CID) has been reported. These fragments have been used for the quantification of almost all pharmaceutical drugs and their metabolites in blood, hair, and water by LC-ESI-MS (Ionita and Akhlaghi 2010, Haneef et al., 2013, Blue et al., 2018). Several drugs form sodium adducts more efficiently compared to protonated ones (Kruve et al., 2013). Additionally, the sodium ion also forms dimers and trimers such as $[2\ M + Na]^+$, $[3\ M + Na]^+$, $[2\ M-2H + Na]^-$ in positive and negative ionization modes, respectively (Stefansson et al., 1996, Muller et al., 2014, Saidykhan et al., 2014).

In previous studies, the ionization behavior in ESI and the fragmentation pattern of alkali metal adducts of a few natural products and drugs are reported (Enke 1997, Wang and Cole 2002, Hong et al., 2017). However, there is no detailed study available specifically for the adduct formation of steroidal drugs and their distinct fragmentation pattern during ESI-MS/MS analysis. Therefore, the present study explores the effect of different metal complexation on the fragmentation patterns of steroidal drugs. Three alkali metals, i.e., Li^+, Na^+, and K^+ commonly found in adducts, were employed to form complexes, subjected to CID QTOF mass spectrometers. We studied the diagnostic fragment patterns of each drug, and proposed fragmentation pathways were verified by calculating their activation energies through density functional theory (DFT). ESI-MS/MS in combination with DFT software has proved to be an essential tool in the structural elucidation of different compounds. These results lead to the ionization of analytes of interest as adducts of alkali metals during ESI-MS ion source operation.

2. Materials and methods

2.1. Chemicals and reagents

Analytical grade and pure (>98%) solvents and chemicals were used in this study. Ultrapure.

filtered deionized water (with resistivity 18.1MΩcm at 25 °C) acquired through Barnstead MicroPure Water Purification System (Thermo Scientific, USA). Methanol was purchased from Merck KGaA, 64,271 (Darmstadt, Germany), formic acid from Daejung (Daejung Chemicals and Metals Co. Ltd, (Korea), acetonitrile from Merck KGaA, 64,271 (Darmstadt, Germany). Sodium chloride (NaCl) was purchased from BioM Laboratories (Cerritos, USA). Lithium chloride (LiCl) was purchased from Sigma-Aldrich, and Potassium chloride (KCl) was purchased from BioM Laboratories (Cerritos, USA). Pharmaceutical drug standards were obtained from the Drug Bank of Dr. Panjwani Center for Molecular Medicine and Drug Research (PCMD), International Centre for Chemical and Biological Sciences (ICCBS), University of Karachi, Karachi, Pakistan. Lithium chloride and sodium chloride were purchased from Samchun Pure Chemical (Pyeongtaek, Korea). Potassium chloride was obtained from Junsei Chemical (Tokyo, Japan).

2.2. Preparation of standard solution and salts solutions

One mg of each standard drug was weighed and dissolved in 1 mL of methanol. One mM solution of each salt was prepared in water at a concentration of 0.1 mM of each salt was pre-

pared by dilution and added to 1000 ng/mL solution of each drug before being subjected to the mass spectrometer.

2.3. Mass spectrometry analysis

Tandem mass spectra of cationized steroidal drugs were obtained using Bruker amaZon speed Ion trap mass spectrometer (Bremen, Germany) in positive ion mode. Samples were injected into the ion trap mass spectrometer with a syringe pump at a flow rate of 5 μL/min; the electrospray voltage and capillary temperature were set to 4.0 kV and 200 °C respectively. Ion source parameters were as follows: capillary voltage at 4500 V (-3500 V for negative mode), endplate offset at 500 V, nebulizer gas 40.0 psi, drying gas at 8.0 L/min, and drying gas temperature at 200 °C. Mass spectra scan range was set at m/z 50 to 1000 while the number of spectral averages was set at 5. Fragmentation was performed under CID, and amplitude was optimized for each analyte to obtain the maximum abundance of fragment ions.

A Bruker maXis II HR-QTOF mass spectrometer (Bremen, Germany) was used to assign fragments and obtain accurate m/z values. Samples were injected into the QTOF mass spectrometer with a syringe pump at a flow rate of 5 μL/min; the electrospray voltage and capillary temperatures were 4.0 kV and 200 °C, respectively. Spectra of all samples were acquired over 200 scans and averaged.

2.4. Computational analysis

Standard quantum chemical calculations were carried out using density functional theory (DFT) with the Gaussian 09 suite of programs. Geometrical parameters of the structures were optimized using the B3LYP hybrid functional method with the 6–31 + + (d)(p) basis set. No symmetry constraints were imposed in the optimization. Initial models for each structure were obtained by placing a metal ion at each putative adduct site, followed by geometry optimization. Zero-point energy corrections were applied to all candidate structures. The more energetically more favorable structures were used in this study. All calculations are done in the gas phase and at a temperature of 300 k.

3. Results and discussion

The tandem mass spectrometry data of steroidal drugs and their alkali metals help us to understand the behavior of fragmentation of steroidal drugs with metal complexes during ESI-MS/MS.

3.1. Fragmentation patterns of drug adducts

Fragmentation pathways of the cationized drugs were investigated using low-energy collision dissociation ESI tandem mass spectrometry (ESI-MS/MS) experiments. Collision energy (CE) optimization was performed by selecting CE between 25 and 60 eV. Low CE (< 25 eV) caused a decrease in the production of the characteristic fragments, while an increase in the CE (> 60 eV) has not provided any further significant information related to characteristic ions that appeared in the MS/MS spectrum because during high collision energy so much noise is produced, and its main fragments could not be easily identified.

The CID-MS/MS of both the precursor protonated molecular ion at m/z 431.2418 and lithiated adduct at m/z 437.2518 of the budesonide steroid created seven product ions at m/z 413.2318, 395.2207, 341.1747, 323.1638, 305.1529, 263.1425, 293.1543 and 365.1931, 419.2402, 349.1979, 331.2088, 251.1614, 209.1507, 143.1042, whereas the precursor sodiated and potassiated adduct at m/z 453.2241 and m/z 469.1975 created seven product ions at m/z 397.2024, 383.1855, 379.1914, 365.1751, 355.1913, 337.1801, 319.1689, 163.1130 and 395.1252, 383.1621, 337.1207, 321.1089, 263.0688. The loss of the H_2O and $C_4H_8O_2$ are common for both sodiated and lithiated adducts as compared to potassiated adducts while other fragments are different for each adduct. The differentiations are obtained in the breaking of C-C bonds between each adduct. The hemiacetal group attached at C16 and C17 is broken in all adducts. The fragments BU1 and BU3 were only observed for lithiated adducts, and BU2 was for sodiated adduct while the BU4 protonated and lithiated adducts. BU5 was observed for protonated, lithiated, and potassiated adducts. The CID-MS/MS of both the precursor protonated molecular ion at m/z 415.2151 and lithiated adduct at m/z 421.2186 of the eplerenone steroid created nine product ions at m/z 397.2024, 383.1855, 379.1914, 365.1751, 355.1913, 337.1801, 319.1689, 163.1130 and seven at m/z 377.1921, 403.2086, 385.1986, 359.1835, 349.1975, 343.1874, 331.1898 respectively, whereas the precursor sodiated and potassiated adduct at m/z 437.1929 and m/z 453.1669 created six product ions at m/z 407.1818, 419.1820, 377.1719, 355.1911, 303.1356, 169.0617 and three product ions at m/z 435.1471, 341.1154, 379.1309, 323.1049 respectively. The loss of H_2O and $2H_2O$ is common for each adduct. The C-C fragments EP1 and EP2 were obtained only in the spectrum of potassiated adduct, while the EP2 and EP5 were only for sodiated adduct and EP4 only for lithiated adduct. The EP6 product ion was observed in the spectrum of all adducts. The CID MS/MS spectrum of fluoxymesterone showed seven fragments in the protonated molecule, six in lithiated adduct, six in sodiated adduct, and four in potassiated adduct. The loss of water (FL5) and/or hydrofluoric acid was observed in the spectrum of the protonated molecule, and all adducts. The product ion FL2 was observed for protonated and lithiated adducts, while FL3 and FL4 were unique fragments in the potassiated spectrum and the FL1 was observed in the sodiated adducts. The CID-MS/MS of the protonated oxandrolone at m/z 307.2258 afforded three major product ions respectively at m/z 289.2162, 271.2062, 247.1693 and the lithium adduct with m/z created four fragments at m/z 295.2244, 269.2087, 243.1931, 173.1153 while the sodiated and potassiated adducts at m/z 329.2091 and 345.1832 respectively created four and two product ions at m/z 311.1982, 285.1825, 259.1669 and 327.1721, 261.1251 respectively. The loss of water molecule (OX1) is common for all metallic adducts. The OX2, OX4, and OX5 product ions were observed for both protonated molecule and lithiated adduct, while the OX3 was observed in the sodiated adduct. The OX6 product ion was observed for protonated and all metal adducts. Both protonated molecule and a lithiated adduct of dienogest created five fragments, three for sodiated adduct, and only one product ion for potassiated adduct. The loss of H_2O (DI7) was common in all adducts and the loss of HCN (DI6) was observed in sodiated

Table 1 MS and MS/MS analysis of steroidal drugs.

Compound Name	Precursor/ Adduct ion	Molecular formula	Observed Values (m/z)	Theo. m/z	Error (ppm)	Collision Energy	MS/MS
Budesonide	$[M + H]^+$	$C_{25}H_{34}O_6 + H^+$	431.2418	431.2434	3.712	25	413.2318, 395.2207, 341.1747, 323.1638, 305.1529, 263.1425, 293.1543
	$[M + Li]^+$	$C_{25}H_{34}O_6 + Li^+$	437.2518	437.2510	1.83	30	365.1931, 419.2402, 349.1979, 331.2088, 251.1614, 209.1507, 143.1042
	$[M + Na]^+$	$C_{25}H_{34}O_6 + Na^+$	453.2241	453.2248	1.54	35	381.1671, 341.1728, 395.2197, 435.2135, 209.0931, 321.1475
	$[M + K]^+$	$C_{25}H_{34}O_6 + K^+$	469.1975	469.1987	2.55	40	395.1252, 383.1621, 337.1207, 321.1089, 263.0688, 321.0888
Eplerenone	$[M + H]^+$	$C_{24}H_{30}O_6 + H^+$	415.2151	415.2115	2.61	27	397.2024, 383.1855, 379.1914, 365.1751, 355.1913, 355.1913, 337.1801, 319.1689, 163.1130
	$[M + Li]^+$	$C_{24}H_{30}O_6 + Li^+$	421.2186	421.2197	2.61	28	377.1921, 403.2086, 385.1986, 359.1835, 349.1975, 343.1874, 331.1898
	$[M + Na]^+$	$C_{24}H_{30}O_6 + Na^+$	437.1929	437.1935	1.37	32	407.1818, 419.1820, 377.1719, 355.1911, 303.1356, 355.1909, 169.0617
	$[M + K]^+$	$C_{24}H_{30}O_6 + K^+$	453.1669	453.1674	1.10	50	435.1471, 341.1154, 379.1309, 323.1049
Fluoxymesterone	$[M + H]^+$	$C_{20}H_{29}FO_3 + H^+$	337.2171	337.2179	2.37	25	319.2073, 301.1980, 317.2113, 299.2011, 281.1905, 241.1590, 181.1020
	$[M + Li]^+$	$C_{20}H_{29}FO_3 + Li^+$	343.2250	343.2255	1.46	26	325.2167, 323.2184, 257.1518, 257.1518, 307.2044, 175.1110
	$[M + Na]^+$	$C_{20}H_{29}FO_3 + Na^+$	359.1987	359.1993	1.67	40	341.1876, 339.1942, 323.1771, 259.1112, 245.0952, 133.0631
	$[M + K]^+$	$C_{20}H_{29}FO_3 + K^+$	375.1738	375.1732	1.60	48	359.1411, 357.1624, 299.0851, 163.0533
Oxandrolone	$[M + H]^+$	$C_{19}H_{30}O_3 + H^+$	307.2258	307.2268	3.25	20	289.2162, 271.2062, 247.1693
	$[M + Li]^+$	$C_{19}H_{30}O_3 + Li^+$	313.2346	313.2350	1.28	24	295.2244, 269.2087, 243.1931, 173.1153
	$[M + Na]^+$	$C_{19}H_{30}O_3 + Na^+$	329.2091	329.2087	1.12	42	311.1982, 285.1825, 259.1669
	$[M + K]^+$	$C_{19}H_{30}O_3 + K^+$	345.1832	345.1827	1.45	45	327.1721, 261.1251
Dienogest	$[M + H]^+$	$C_{20}H_{25}NO_2 + H^+$	312.1947	312.1964	5.44	20	294.1854, 285.1853,271.1693, 253.1588, 161.0961
	$[M + Li]^+$	$C_{20}H_{25}NO_2 + Li^+$	318.2051	318.2040	3.46	26	300.1936, 291.1913, 277.1941, 233.1519, 153.0872
	$[M + Na]^+$	$C_{20}H_{25}NO_2 + Na^+$	334.1769	334.1778	2.69	33	316.1668, 307.1678, 197.0941
	$[M + K]^+$	$C_{20}H_{25}NO_2 + K^+$	350.1521	350.1517	1.14	42	265.0983
Finasteride	$[M + H]^+$	$C_{23}H_{36}N_2O_2 + H^+$	373.2844	373.2850	1.60	26	355.2752, 317.2225
	$[M + Li]^+$	$C_{23}H_{36}N_2O_2 + Li^+$	379.2931	379.2931	3.46	29	306.2046, 200.1627, 142.0835, 288.1939
	$[M + Na]^+$	$C_{23}H_{36}N_2O_2 + Na^+$	395.2672	395.2669	0.75	40	256.1677, 216.1366, 324.1943, 266.1512
	$[M + K]^+$	$C_{23}H_{36}N_2O_2 + K^+$	411.2403	411.2408	1.22	44	338.1519, 110.0001
Etonogestrel	$[M + H]^+$	$C_{22}H_{28}O_2 + H^+$	325.2175	325.2162	3.99	30	307.2059, 299.2009, 257.1902
	$[M + Li]^+$	$C_{22}H_{28}O_2 + Li^+$	331.2253	331.2244	2.71	36	303.1938, 143.1039, 313.2132, 287.1979
	$[M + Na]^+$	$C_{22}H_{28}O_2 + Na^+$	347.1979	347.1982	0.86	49	329.1868, 289.1562, 119.0459, 321.1831
	$[M + K]^+$	$C_{22}H_{28}O_2 + K^+$	363.1724	363.1721	0.83	50	111.0201, 307.1449, 189.0672, 149.0360, 213.0671
Norethisterone	$[M + H]^+$	$C_{20}H_{26}O_2 + H^+$	299.2006	299.2011	1.67	27	281.1800, 231.1746, 215.1421
	$[M + Li]^+$	$C_{20}H_{26}O_2 + K^+$	305.2075	305.2087	3.93	30	235.1671, 99.0419, 287.1976, 263.1969, 167.1036
	$[M + Na]^+$	$C_{20}H_{26}O_2 + Na^+$	321.1836	321.1825	3.42	41	303.1711, 261.1261, 293.1521, 223.1082, 199.1079
	$[M + K]^+$	$C_{20}H_{26}O_2 + K^+$	337.1557	337.1564	2.08	45	265.0979, 263.0824
Estradiol Dipropionate	$[M + H]^+$	$C_{24}H_{32}O_4 + H^+$	385.2371	385.2379	2.07	30	329.2112, 313.2162, 311.2009, 255.1743, 157.1222
	$[M + Li]^+$	$C_{24}H_{32}O_4 + Li^+$	391.2459	391.2455	1.02	30	335.2187, 317.2075, 317.2075, 159.0985
	$[M + Na]^+$	$C_{24}H_{32}O_4 + Na^+$	407.2183	407.2193	2.46	35	391.1876, 349.1764, 333.1822
	$[M + K]^+$	$C_{24}H_{32}O_4 + K^+$	423.1949	423.1932	4.01	40	349.1554, 365.1509
Cortisone	$[M + H]^+$	$C_{21}H_{28}O_5 + H^+$	361.2008	361.2015	1.93	33	343.1901, 300.1711, 163.1111, 265.1449, 241.1436
	$[M + Li]^+$	$C_{21}H_{28}O_5 + Li^+$	367.2086	367.2091	1.36	35	337.1976, 349.1967, 235.1313
	$[M + Na]^+$	$C_{21}H_{28}O_5 + Na^+$	383.1828	383.1829	0.62	40	351.1559, 255.1346, 365.1739, 323.1621
	$[M + K]^+$	$C_{21}H_{28}O_5 + K^+$	399.1572	399.1568	1.00	44	383.1263, 381.1445
Norethisterone Acetate	$[M + H]^+$	$C_{22}H_{28}O_3 + H^+$	341.2109	341.2117	2.34	33	299.2013, 281.1902, 231.1752, 231.1752, 281.1902
	$[M + Li]^+$	$C_{22}H_{28}O_3 + Li^+$	347.2187	347.2193	1.73	33	305.2073, 303.1942, 287.1973, 263.1969

Table 1 (*continued*)

Compound Name	Precursor/ Adduct ion	Molecular formula	Observed Values (m/z)	Theo. m/z	Error (ppm)	Collision Energy	MS/MS
	$[M + Na]^+$	$C_{22}H_{28}O_3 + Na^+$	363.1943	363.1931	3.30	45	229.1569, 303.1713, 263.1412, 129.0322
	$[M + K]^+$	$C_{22}H_{28}O_3 + K^+$	379.1669	379.1670	0.62	55	353.1509, 135.0209, 319.1454, 335.1412
Prednisolone	$[M + H]^+$	$C_{21}H_{28}O_5 + H^+$	361.2012	361.2015	0.83	25	343.1909, 325.1806, 307.1698, 265.1599, 173.0962
	$[M + Li]^+$	$C_{21}H_{28}O_5 + Li^+$	367.2096	367.2091	1.36	27	349.1989, 337.1976, 319.1879, 307.1877, 281.2094, 331.1888
	$[M + Na]^+$	$C_{21}H_{28}O_5 + Na^+$	383.1821	383.1829	2.09	46	365.1716, 323.1609, 255.1365
	$[M + K]^+$	$C_{21}H_{28}O_5 + K^+$	399.1549	399.1568	4.76	54	313.1553, 381.1451, 363.1331
Prednisolone Acetate	$[M + H]^+$	$C_{23}H_{30}O_6 + H^+$	403.2109	403.2121	2.97	27	345.2058, 331.1908, 307.1551, 385.2020, 367.1913
	$[M + Li]^+$	$C_{23}H_{30}O_6 + Li^+$	409.2187	409.2197	2.44	39	195.0987, 367.2096, 153.0894, 391.2085, 331.1871, 349.1976, 305.1735, 251.1610, 313.1784
	$[M + Na]^+$	$C_{23}H_{30}O_6 + Na^+$	425.1921	425.1935	3.29	49	279.1356, 407.1831, 363.1553, 365.1719, 383.1816
	$[M + K]^+$	$C_{23}H_{30}O_6 + K^+$	441.1664	441.1674	2.26	55	425.1373, 423.1551, 405.1474
Pregnenolone	$[M + H]^+$	$C_{21}H_{32}O_2 + H^+$	317.2471	317.2481	3.15	30	299.2369, 273.2306, 255.2111, 281.2268, 159.1169
	$[M + Li]^+$	$C_{21}H_{32}O_2 + Li^+$	323.2564	323.2557	2.17	35	305.2447, 227.1967, 209.1505, 113.0564
	$[M + Na]^+$	$C_{21}H_{32}O_2 + Na^+$	339.2283	339.2295	3.54	45	279.1712, 117.0307, 321.2191, 281.1887, 227.1412
	$[M + K]^+$	$C_{21}H_{32}O_2 + K^+$	355.2030	355.2034	1.12	50	267.1139, 231.1152, 337.1912, 111.0201

and lithiated adducts. The C-C breaking fragment DI4 was only observed in the potassiated adducts while DI2 was only observed for sodiated. DI3 was observed in lithiated adducts and DI5 for both, protonated and lithiated adducts. Finasteride showed two product ions in protonated molecule spectrum, four in lithiated adduct, five in sodiated adduct, and three in potassiated adduct. The loss of water (FI7) was observed only in the protonated ones, while FI1 product ion was observed only in the potassiated spectrum, FI2 in sodiated adduct, and FI3 in the lithiated adduct. The FI2 and FI3 were obtained in the spectrum of both lithiated and sodiated adducts. The protonated molecule of etonogestrel showed three product ions, lithiated and sodiated adducts produced four product ions and potassiated adduct produced six ions. The product ion (ET6) indicates water loss observed in protonated, lithiated and sodiated adducts. Loss of acetylene (ET5) was observed for all adducts. The ET4 and ET3 were observed only in the spectrum of potassiated adduct, while the ET1 product ion observed for sodiated adduct and ET2 were only observed and lithiated adduct. The protonated ion of norethisterone showed three fragments, lithiated and sodiated adducts showed five product ions, and potassiated adduct produced two ions. The water loss (NO5) is observed for protonated, sodiated, and lithiated adducts. NO1 and NO4 product ions were obtained only in the spectrum of the sodiated adduct. The product ion NO3 was also observed for both protonated molecule and potassiated adduct. The CID-MS/MS of both the precursor protonated molecular ion at m/z 385.2371 and lithiated adduct at m/z 391.2459 of the estradiol dipropionate steroid created five and four product ions respectively while the sodiated and potassiated at m/z 407.2183 and 423.1949 created three and two product ions respectively. The losses of the carboxylic group (ED2) and aldehyde (ED3) groups were observed for all the adducts. The product ion ED1 was observed for both protonated and lithiated adducts, while ED4 was only observed in sodiated adducts. Cortisone showed six major product ions in the spectrum of the protonated adduct, three in lithiated adduct, four in sodiated adduct, and two in the potassiated adduct spectrum. The loss of water (CO5) is common for each molecular ion peak, and the loss of CH_2O molecule (CO4) is observed in the spectra of lithiated and sodiated adducts. The product ions CO3 and CO6 were observed for protonated molecule, sodiated and potassiated adducts, respectively. Norethisterone acetate showed four fragments in the spectrum of all protonated, lithiated, sodiated, and potassiated adducts. The product ion NA3, the loss of acetic acid, was observed in the protonated molecule and all adducts. The product ion NA2 and NA5 were observed in the spectrum of both sodiated and potassiated adducts. MS/MS spectrum of the protonated molecule of prednisolone showed four product ions, lithiated adducts showed six product ions, and both sodiated and potassiated adducts showed three product ions. The loss of water (PD4) and $C_2H_4O_2$ loss were observed in the lithiated and sodiated adducts. The product ion PD3 was observed only in the lithiated adduct. The protonated, lithiated adduct, sodiated adduct, and potassiated adduct of prednisolone acetate showed five, nine, seven, and four product ions respectively. The loss of water (PA6) is observed in the spectrum of all adducts. The product ions PA4 and PA5 were observed in the spectrum of both lithiated and sodiated adducts. The product ion PA1 was obtained only in the sodiated adduct spectrum, the PA2 in the lithiated adduct, the PA3 in the protonated molecule, and the PA7 in the potassiated adduct. The CID-MS/MS of both the precursor protonated molecular ion at m/z 317.2471 and lithiated adduct at m/z 323.2564 of the pregnenolone steroid created

Budesonide Fragments
BU1, 143 Da (Li)
BU2, 209 Da (Na)
BU3, 209 Da (Li)
BU4, 341 Da (H), 349 (Li)
BU5, 413 (H), 419 (Li), 435 (Na) Da

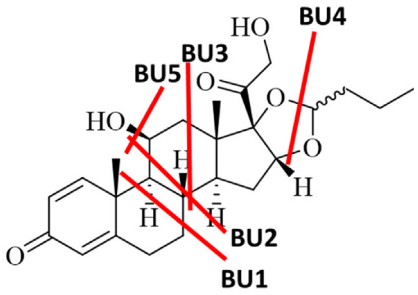

Eplerenone Fragments
EP1, 341 (K) Da
EP2, 355 (H), 377 (Na) Da
EP3, 377(Li) Da
EP4, 379 (K) Da
EP5, 383 (H), 407 (Na) Da
EP6, 397 (H), 403 (Li), 419 (Na) 435 (K) Da

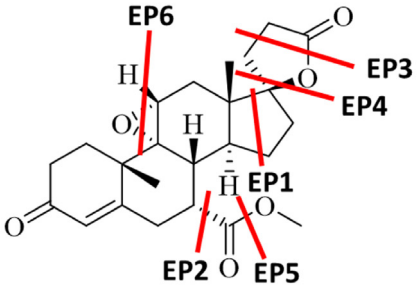

Fluoxymesterone Fragments
FL1, 133 (Na) Da
FL2, 181 (H), 187 (Li) Da
FL3, 299 (K) Da
FL4, 359 (K) Da
FL5, 319 (H), 325 (Li), 341 (Na) 357 (K) Da

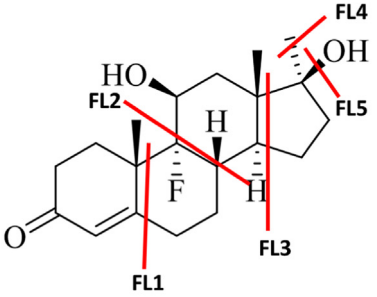

Oxandrolone Fragments
OX1, 173 (Li) Da
OX2, 243 (Li) Da
OX3, 247 (H) Da
OX4, 269 (Li), 285 (Na) Da
OX5, 270 (H) Da
OX6, 288 (H), 295 (Li), 311 (Na) 327 (K) Da

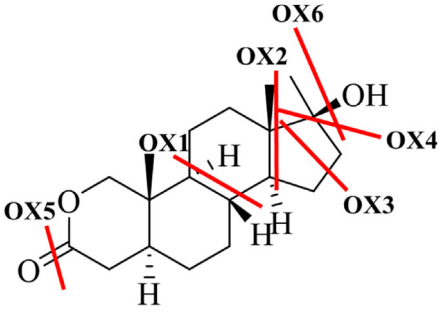

Dienogest Fragments
DI1, 161 (H) Da
DI2, 197 (Na) Da
DI3, 233 (Li) Da
DI4, 265 (K) Da
DI5, 271 (H), 277 (Li) Da
DI6, 285 (H), 291 (Li), 307 (Na) Da
DI7, 294 (H), 300 (Li), 316 (Na) Da

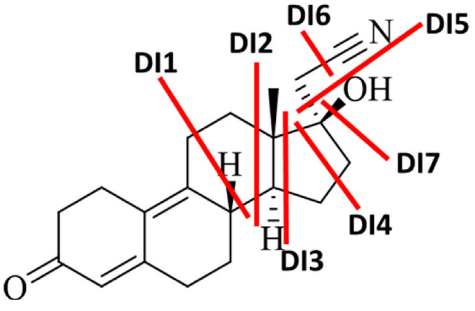

Fig. 1 The proposed C-C bond fragments of all drugs in each adduct.

four product ions while the sodiated and potassiated at m/z 339.2283 and 355.2030 created three and two product ions respectively. The loss of water (PG4) is common for all adducts. The product ion PG1 is observed only in the spectrum of potassiated adduct, product ion PG2 in the protonated, spectrum, and product ion PG3 in the sodiated spectrum.

The tandem mass spectral data of all drugs are presented in Table 1. The losses, product ions, and their elemental composition of all adducts of all steroids are presented in Fig. 1 and Supplementary Scheme 1–14.

Finasteride Fragments
FI1, 110 (K) Da
FI2, 142 (Li), 158 (Na) Da
FI3, 200 (Li) 216 (Na) Da
FI4, 256 (Na) Da
FI5, 306 (Li) Da
FI6, 317 (H), 338 (K) Da
FI7 355 (H) Da

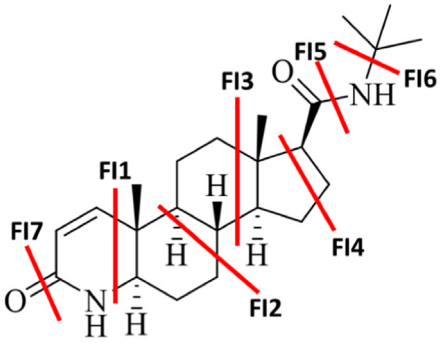

Etonogestrel Fragments
ET1, 119 (Na) Da
ET2, 142 (Li) Da
ET3, 189 (K) Da
ET4, 213 (K) Da
ET5, 249 (H), 303 (Li), 321 (Na) 345 (K) Da
ET6, 307 (H), 313 (Li), 329 (Na) Da

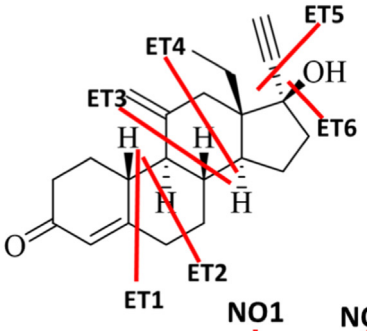

Norethisterone Fragments
NO1, 199 (Na) Da
NO2, 215 (H) Da
NO3, 231 (H), 265 (K) Da
NO4, 293 (Na) Da
NO5, 281 (H), 287 (Li), 303 (Na) Da

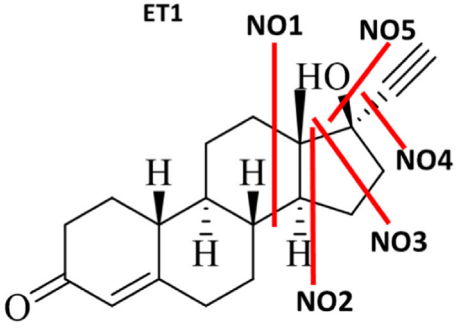

Estradiol Dipropionate Fragments
ED1, 157 (H), 159 (Li) Da
ED2, 313 (H), 317 (Li), 333 (Na) 349 (K) Da
ED3, 329 (H), 335 (Li), 349 (Na), 365 (K) Da
ED4, 391 (Na) Da

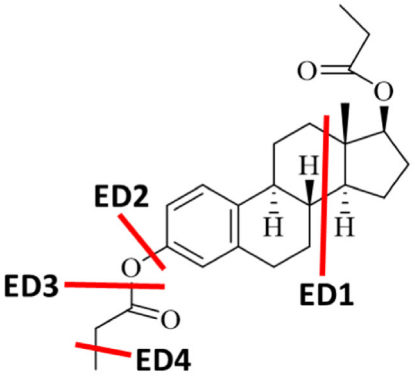

Cortisone Fragments
CO1, 165 (H) Da
CO2, 241 (H) Da
CO3, 301 (H), 323 (Na) Da
CO4, 337 (Li), 353 (Na) Da
CO5, 343 (H), 349 (Li), 363 (Na), 381 (K) Da
CO6, 345 (H), 383 (K) Da

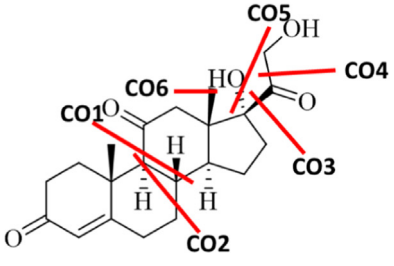

Fig. 1 (*continued*)

Norethisterone Acetate Fragments
NA1, 353 (K) Da
NA2, 299 (H), 303 (Li), 335 (K) Da
NA3, 281 (H), 287 (Li), 303 (Na), 319 (K) Da
NA4, 231 (H) Da
NA5, 119 (Na), 135 (K) Da

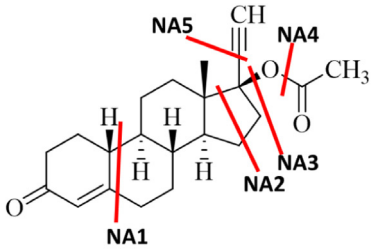

Prednisolone Fragments
PD1, 181 (LI), 313 (K) Da
PD2, 307 (Li), 323 (Na) Da
PD3, 337 (Li) Da
PD4, 343 (H), 349 (Li), 365 (Na), 381 (K) Da

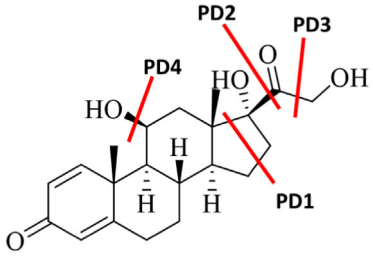

Prednisolone Acetate Fragments
PA1, 185 (Na) Da
PA2, 195 (Li) Da
PA3, 331 (H) Da
PA4, 349 (Li), 365 (Na) Da
PA5, 367 (Li), 383 (Na) Da
PA6, 385 (H), 391 (Li), 407 (Na), 423 (K) Da
PA7 425 (K) Da

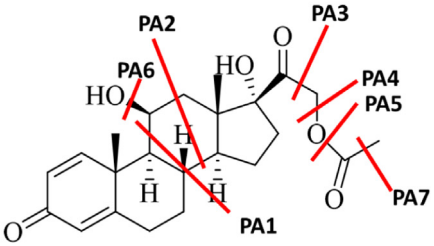

Pregnenolone Fragments
PG1, 231 (K) Da
PG2, 279 (H) Da
PG3, 283 (Na) Da
PG4, 299 (H), 305 (Li), 321 (Na), 337 (K) Da

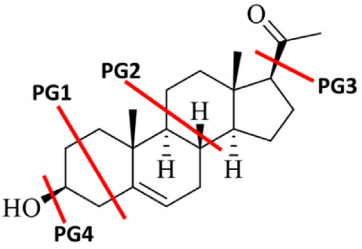

Fig. 1 (*continued*)

Table 2 Binding energies of each cationized drug.

Relative binding energy (kJ/mol)	H^+	Li^+	Na^+	K^+
Budesonide	−1417.11	−1424.02	−1577.90	−2013.44
Eplerenone	−1376.87	−1383.82	−1537.66	−1973.30
Fluoxymesterone	−1099.58	−1106.54	−1260.37	−1696.00
Oxandrolone	−963.03	−970.6267	−1117.12	−1559.41
Dienogest	−977.54	−984.47	−1138.29	1573.92
Finasteride	−1152.29	−1259.31	−1313.08	−1748.67
Etonogestrel.	−1000.62	−1007.56	−1161.35	−1596.95
Norethisterone	−923.66	−930.58	−1084.40	−1518.41
Estradiol Dipropionate	−1228.56	−1227.60	−1381.06	−1824.89
Cortisone	−1187.21	−1194.10	−1347.86	−1783.51
Norethisterone Acetate	−1075.49	−1082.40	−1236.23	−1671.14
Prednisolone	−1187.21	−1194.12	−1347.92	−1783.55
Prednisolone Acetate	−1339.01	1345.96	−1499.74	−1674.02
Pregnenolone	−965.20	−972.16	−1125.96	−1561.59

3.2. Effects of the alkali-metal ions cationization on structures and fragmentation, and computational studies

We have investigated the structural characteristics of selected alkali metal cations and their distinct fragmentation patterns. Different calculation methods were used to predict the position of the proton or the alkali metal ions in the complexes and reasonable fragmentation. To locate the position of the proton and alkali metal in all steroidal drugs, we have carried out a series of DFT calculations using the Gaussian 09 program (Frisch et al., 2016) suit at the B3LYP level of theory with the 6–31 + + G(d) basis set. The minimum energy conformation of the neutral molecules was first optimized, and every possible site was then individually protonated and metalized after optimization. There are different possible protonation metalized sites, the oxygen's, nitrogen groups, and it was found that all drugs showed minimum energy for protonation at carbonyl oxygen atom. In contrast, the metals showed binding with more than two electronegative atoms in all molecules. For example, in oxandrolone, it was found that the carbonyl oxygen (O-1) displayed minimum energy for protonation, while the metal showed binding with (O-1) and (O-2) with minimum energy. In the dienogest, etonogestrel, and pregnenolone metal cation interacts with metal showed binding with carbonyl oxygen (O-1) with minimum energy. In finasteride, the carbonyl oxygen (O-1) showed minimum energy for protonation. In contrast, the metal showed binding with (O-1) and (N-1) with minimum energy. In estradiol dipropionate, the protonation occurs at carbonyl oxygen atoms of the COO group while the metals showed minimum energy to attach with the ester group at C3 of ring A. In cortisone, the carbonyl oxygen (O-1) showed minimum energy for protonation while the metal showed binding with (O-3), (O-4), and (O-5) at C-17, C-20, and C-21 atoms, respectively. In prednisolone and prednisolone acetate, the carbonyl oxygen (O-1) showed minimum energy for protonation while the metal showed binding with (O-1), (O-3), and (O-6) with minimum energy (see Supplementary Scheme-15).

Geometries of the optimized structures, mechanisms of key fragments, and possible routes of all drug's adducts were proposed. The binding energy of metal with molecules decreases as size increases from Li^+, Na^+, and K^+. The fragmentation patterns observed for these Li^+, Na^+, and K^+ ions are different. The number of fragments decreases as the metal size increases, suggesting the difference in binding position and strength of interaction of the molecule with metal cations. The proton can be readily bound to electronegative groups or atoms. However, for the molecules cationized by the metal ions, the positions of the metal are different.

Moreover, the bond lengths of protonated and metallated, and non-cationized forms were investigated. A comparison of bond lengths between all forms showed considerable bond elongation in the vicinity of the protonation and metallated site, thereby leading to the characteristic fragments. The lengths of dissociable bonds are the highest in lithium among the alkali metal complexes of all compounds. Lithium-ion's ion–dipole interactions induce the elongation of bonds more than other metals. The lithium adducts of all drugs have more fragments than other adducts due to the greater lengths of dissociable bonds (Table 3) and lower binding energy (Table 2). The highest ion–dipole interactions of lithium induce the elongation of the C–O bonds of the hydroxyl group and other C-C

Table 3 Bond lengths of dissociable bonds in all metalated drugs.

Name	Dissociable bonds (Å)	H^+	Li^+	Na^+	K^+
Budesonide	C17-O1	1.496	1.492	1.454	1.434
	C16-O2	1.424	1.599	1.459	1.437
	C11-O3	1.420	1.474	1.447	1.429
Eplerenone	C11-O1	1.528	1.520	1.478	1.464
	C9-O1	1.506	1.503	1.484	1.467
Fluoxymesterone	C17-O1	1.585	1.554	1.533	1.492
	C9-F1	1.486	1.479	1.444	1.435
Oxandrolone	C17-O1	1.476	1.448	1.446	1.445
Dienogest	C17-O1	1.451	1.449	1.445	1.443
Finasteride	C20-N2	1.380	1.380	1.671	1.691
	C17-C20	1.528	1.527	1.514	1.515
	N2-C24	1.493	1.491	1.466	1.458
	C17-O1	1.466	1.465	1.463	1.421
	C17-C20	1.476	1.474	1.473	1.470
Etonogestrel	C17-O1	1.483	1.476	1.455	1.442
Norethisterone	C17-O1	1.455	1.465	1.454	1.453
	C17-C20	1.466	1.478	1.469	1.466
Estradiol Dipropionate	C17-O1	1.480	1.453	1.443	1.416
	C21-O1	1.384	1.354	1.349	1.333
Cortisone	C17-O1	1.480	1.593	1.541	1.523
	C17-C20	1.580	1.493	1.488	1.485
Norethisterone Acetate	C17-O1	1.480	1.508	1.486	1.433
	C21-O1	1.540	1.394	1.392	1.371
Prednisolone	C17-O1	1.488	1.476	1.456	1.445
	C17-C20	1.544	1.529	1.524	1.489
Prednisolone Acetate	C17-O1	1.480	1.476	1.472	1.443
	C17-C20	1.534	1.533	1.523	1.502
Pregnenolone	C17-O1	1.526	1.501	1.474	1.467

bonds. Elimination of the water molecule has been observed in the MS2 spectrum of protonated, lithiated, and sodiated ions in every drug with OH. In the potassiated ion, dehydration was not observed for some drugs. It is concluded that the formation of the dehydrated fragment is prevented by the strong ion–dipole interactions between the metal cation and the hydroxyl groups. In potassiated adducts, the metal bounds strongly with the functional –OH group and highly stable adduct.

4. Conclusion

The fragmentation patterns of three different metal adducts of 14 steroidal drugs using ESI MS/MS are presented in this study. The lithiated and protonated adducts of all drugs showed similar fragments. However, the sodiated and potassiated adducts exhibit different fragments. The number of fragments decreases as the metal size increases from Li^+, Na^+, and K^+. Compared to protonated molecules, some metal adducts tend not to produce $[M-H_2O]^+$ ions except lithiated ions. We suggested the structures of the alkali metal complexes of these all drugs formed during ionization in an ESI ion source by using theoretical calculations with DFT. The binding sites of all metals with drugs are different from the proton. The coordination and binding strength of alkali metals to all drugs promote distinct gas-phase structures and fragmentation patterns. The understanding of the relationship between the structure of precursor ions and their fragmentation pathways will improve the quality of the related studies.

Declaration of Competing Interest

The authors declare that they have no known competing financial interests or personal relationships that could have appeared to influence the work reported in this paper.

Acknowledgments

The authors acknowledge the support of Mr. Arsalan Tahir and Mr. Junaid Ul Haq for their technical assistance in the UHPLC-MS/MS analysis. Ms. Batool Fatima and Ms. Hiba Fatima are acknowledged for their help in collecting compounds. The authors would like to extend their appreciation to the Deanship of scientific research at King Khalid University for their support through the research group program (RGP.2/117/42). Mr. Syed Usama Yaseen Jeelani would also like to acknowledge the Higher Education Commission (HEC), Pakistan, for their financial assistance under the HEC Indigenous Ph.D. Fellowship Program [HEC (FD)/2021/5142].

Appendix A. Supplementary data

Supplementary data to this article can be found online at https://doi.org/10.1016/j.arabjc.2022.103939.

References

Bacaloni, A., Cavaliere, C., Faberi, A., et al, 2005. Determination of isoflavones and coumestrol in river water and domestic wastewater sewage treatment plants. Anal. Chim. Acta 531, 229–237. https://doi.org/10.1016/j.aca.2004.10.037.

Blue, S.W., Winchell, A.J., Kaucher, A.V., et al, 2018. Simultaneous quantitation of multiple contraceptive hormones in human serum by LC-MS/MS. Contraception. 97, 363–369. https://doi.org/10.1016/j.contraception.2018.01.015.

Cech, N.B., Enke, C.G., 2001. Practical implications of some recent studies in electrospray ionization fundamentals. Mass Spectrom. Rev. 20, 362–387. https://doi.org/10.1002/mas.10008.

Duan, X., Luo, G., Chen, Y., et al, 2012. Effects of alkali metal ion cationization on fragmentation pathways of triazole-epothilone. J. Am. Soc. Mass Spectrom. 23, 1126–1134. https://doi.org/10.1007/s13361-012-0376-0.

El-Aneed, A., Banoub, J., Koen-Alonso, M., et al, 2007. Establishment of mass spectrometric fingerprints of novel synthetic cholesteryl neoglycolipids: the presence of a unique C-glycoside species during electrospray ionization and during collision-induced dissociation tandem mass spectrometry. J. Am. Soc. Mass Spectrom. 18, 294–310.

Enke, C.G., 1997. A predictive model for matrix and analyte effects in electrospray ionization of singly-charged ionic analytes. Anal. Chem. 69, 4885–4893. https://doi.org/10.1021/ac970095w.

Fang, M., Rustam, Y., Palmieri, M., et al, 2020. Evaluation of ultraviolet photodissociation tandem mass spectrometry for the structural assignment of unsaturated fatty acid double bond positional isomers. Anal. Bioanal. Chem. 412, 2339–2351. https://doi.org/10.1007/s00216-020-02446-6.

Fragkaki, A.G., Angelis, Y.S., Tsantili-Kakoulidou, A., et al, 2009. Statistical analysis of fragmentation patterns of electron ionization mass spectra of enolized-trimethylsilylated anabolic androgenic steroids. Int. J. Mass Spectrom. 285, 58–69. https://doi.org/10.1016/j.ijms.2009.04.008.

Frisch, M. J., G. W. Trucks, H. B. Schlegel, et al., 2016. Gaussian 16 Rev. C.01. Wallingford, CT.

Fujihara, A., Sha, Y., Matsuo, S., et al, 2014. High-energy collision-activated and electron-transfer dissociation of gas-phase complexes of tryptophan with Na+, K+, and Ca2+. European Physical J. D. 68. https://doi.org/10.1140/epjd/e2014-50302-5.

Haneef, J., Shaharyar, M., Husain, A., et al, 2013. Application of LC-MS/MS for quantitative analysis of glucocorticoids and stimulants in biological fluids. J. Pharm. Anal. 3, 341–348. https://doi.org/10.1016/j.jpha.2013.03.005.

Hong, A., Lee, H.H., Heo, C.E., et al, 2017. Distinct Fragmentation Pathways of Anticancer Drugs Induced by Charge-Carrying Cations in the Gas Phase. J. Am. Soc. Mass Spectrom. 28, 628–637. https://doi.org/10.1007/s13361-016-1559-x.

Ionita, I.A., Akhlaghi, F., 2010. Quantification of unbound prednisolone, prednisone, cortisol and cortisone in human plasma by ultrafiltration and direct injection into liquid chromatrography tandem mass spectrometry. Ann. Clin. Biochem. 47, 350–357. https://doi.org/10.1258/acb.2010.010027.

Kasper, P.T., Rojas-Cherto, M., Mistrik, R., et al, 2012. Fragmentation trees for the structural characterisation of metabolites. Rapid Commun. Mass Spectrom. 26, 2275–2286. https://doi.org/10.1002/rcm.6340.

Kim, Y.H., Yoo, J.S., Lee, C.H., et al, 1996. Application of fast atom bombardment combined with tandem mass spectrometry to the structural elucidation of O-demethylabierixin and related polyether antibiotics. J. Mass Spectrom. 31, 855–860.

Kruve, A., Kaupmees, K., Liigand, J., et al, 2013. Sodium adduct formation efficiency in ESI source. J. Mass Spectrom. 48, 695–702. https://doi.org/10.1002/jms.3218.

Lee, S.-W., Kim, H.S., Beauchamp, J.L., 1998. Salt Bridge Chemistry Applied to Gas-Phase Peptide Sequencing: Selective Fragmentation of Sodiated Gas-Phase Peptide Ions Adjacent to Aspartic Acid Residues. J. Am. Chem. Soc. 120, 3188–3195. https://doi.org/10.1021/ja973467r.

Liigand, P., Liigand, J., Kaupmees, K., et al, 2020. 30 Years of research on ESI/MS response: Trends, contradictions and applications. Anal. Chim. Acta 238117. https://doi.org/10.1016/j.aca.2020.11.049.

Muller, C., Kanawati, B., Rock, T.M., et al, 2014. Dimer ion formation and intermolecular fragmentation of 1,2-diacylglycerols revealed by electrospray ionization Fourier transform ion cyclotron resonance mass spectrometry for more comprehensive lipid analysis. Rapid Commun. Mass Spectrom. 28, 1735–1744. https://doi.org/10.1002/rcm.6956.

Musharraf, S.G., Ali, A., Khan, N.T., et al, 2013. Tandem mass spectrometry approach for the investigation of the steroidal metabolism: structure-fragmentation relationship (SFR) in anabolic steroids and their metabolites by ESI-MS/MS analysis. Steroids 78, 171–181. https://doi.org/10.1016/j.steroids.2012.10.017.

Nikolskiy, I., Siuzdak, G., Patti, G.J., 2015. Discriminating precursors of common fragments for large-scale metabolite profiling by triple quadrupole mass spectrometry. Bioinformatics 31, 2017–2023. https://doi.org/10.1093/bioinformatics/btv085.

Perdivara, I., Petrovich, R., Allinquant, B., et al, 2009. Elucidation of O-glycosylation structures of the β-amyloid precursor protein by liquid chromatography− mass spectrometry using electron transfer dissociation and collision induced dissociation. J. Proteome Res. 8, 631–642.

Saidykhan, A., Ayrton, S.T., Gallagher, R.T., et al, 2014. Novel formation of [2M-H](+) species in positive electrospray mass spectra of indoles. Rapid Commun. Mass Spectrom. 28, 1948–1952. https://doi.org/10.1002/rcm.6976.

Selby, T.L., Wesdemiotis, C., Lattimer, R.P., 1994. Dissociation characteristics of [M + X]+ ions (X = H, Li, Na, K) from linear and cyclic polyglycols. J. Am. Soc. Mass Spectrom. 5, 1081–1092. https://doi.org/10.1016/1044-0305(94)85069-0.

Stefansson, M., Sjöberg, P.J.R., Markides, K.E., 1996. Regulation of Multimer Formation in Electrospray Mass Spectrometry. Anal. Chem. 68, 1792–1797. https://doi.org/10.1021/ac950980j.

Uddin, J., Muhsinah, A.B., Imran, M., et al, 2022. Structure-fragmentation study of pentacyclic triterpenoids using electrospray ionization quadrupole time-of-flight tandem mass spectrometry (ESI-QTOFMS/MS). Rapid Commun. Mass Spectrom. 36,. https://doi.org/10.1002/rcm.9243 e9243.

Wang, G., Cole, R.B., 2002. Effect of Solution Ionic Strength on Analyte Charge State Distributions in Positive and Negative Ion Electrospray Mass Spectrometry. Anal. Chem. 66, 3702–3708. https://doi.org/10.1021/ac00093a026.

Wang, P., Polce, M.J., Bleiholder, C., et al, 2006. Structural characterization of peptides via tandem mass spectrometry of their dilithiated monocations. Int. J. Mass Spectrom. 249, 45–59.

Wei, J., Bristow, A.W., O'Connor, P.B., 2015. The Competitive influence of Li+, Na+, K+, Ag+, and H+ on the fragmentation of a PEGylated polymeric excipient. J. Am. Soc. Mass Spectrom. 26, 166–173. https://doi.org/10.1007/s13361-014-1009-6.

Zhu, X., Kalyanaraman, N., Subramanian, R., 2011. Enhanced screening of glutathione-trapped reactive metabolites by in-source collision-induced dissociation and extraction of product ion using UHPLC-high resolution mass spectrometry. Anal. Chem. 83, 9516–9523. https://doi.org/10.1021/ac202280f.